Numerical modeling of HgCdTe solidification: effects of phase diagram, double-diffusion convection and microgravity level.

Andris V. Bune[a], Donald C. Gillies[b] and Sandor L. Lehoczky[b]
[a]National Research Council / Space Science Laboratory, NASA Marshall Space Flight Center, ES 75, Huntsville, Al 35812, USA
[b]Space Science Laboratory, NASA Marshall Space Flight Center, ES 75, Huntsville, Al 35812, USA

ABSTRACT

A numerical model of HgCdTe solidification was implemented using finite the element code FIDAP. Model verification was done using both experimental data and numerical test problems. The model was used to evaluate possible effects of double-diffusion convection in molten material, and microgravity level on concentration distribution in the solidified HgCdTe. Particular attention was paid to incorporation of HgCdTe phase diagram. It was found, that below a critical microgravity amplitude, the maximum convective velocity in the melt appears virtually independent on the microgravity vector orientation. Good agreement between predicted interface shape and an interface obtained experimentally by quenching was achieved. The results of numerical modeling are presented in the form of video film.

Keywords: Binary alloy, HgCdTe, bulk crystal growth, directional solidification, microgravity, numerical modelling, FIDAP.

1. INTRODUCTION

Solidification of HgCdTe was the subject of recent numerical modeling [1-4]. In these papers particular attention was paid to proper modeling of melt convection and solidification to predict the crystal/melt interface shape and crystal radial and axial inhomogenity. In order to achieve this, HgCdTe was considered as binary alloy with melting temperature available from phase diagram. The present study is a continuation of these efforts with the emphasis on investigation of melt convection on microgravity level, double-diffusion and interface shape. It is useful to clarify from the beginning, that information about actual crystal / melt interface during growth process is available *a posteriori*, and can be obtained from radial distribution of mole concentration of CdTe and from visible change in crystal morphology, that occurs if the growth process is interrupted by fast sample removal from the furnace (quench). No direct information about convection velocity is available. In the present work double diffusion convection in HgCdTe melt and crystal-melt interface curvature prediction during directional solidification are addressed numerically using the finite element approach.

It appears that both global modeling of heat transfer in the furnace along with a detailed solidification model are required to fulfill proper modeling of crystal growth as well as furnace. A global model of AADSF furnace[5], that includes radiative, conductive and convective heat transfer was used to obtain the appropriate temperature boundary conditions for detailed solidification model. Alternatively experimental temperature measurements were used to generate temperature boundary conditions for the numerical model. The numerical model of convection and solidification of binary alloy is based on the general equations of heat and mass transfer in two-dimensional region. Minimal code development was undertaken, as commercial finite element code FIDAP [6] was used. Two complimentary solutions where obtained: one for melt region with a fixed boundary and other for melt region with an unknown boundary. In the former case, numerically converged solutions where typically easily obtained with standard FIDAP settings, while in the latter case a special choice of relaxation factors for each degree of freedom was required. The simplified model with

PROCEEDINGS REPRINT

SPIE—The International Society for Optical Engineering

Reprinted from

Materials Research in Low Gravity

28–29 July 1997
San Diego, California

Volume 3123

fixed interface shape was especially useful for parametric study of convection, as the steady state solution was available for a broad range of parameters.

In the complete numerical model with unknown boundary the following thermophysical properties of HgCdTe was taken into account: the pseudobinary HgTe-CdTe phase diagram[7], the compositional dependence of the interface segregation coefficient, an assumed diffusion coefficient for mass transport in HgCdTe, the temperature and composition dependence of the melt density (to calculate buoyancy force) and the melt viscosity and its temperature dependence[8]. The composition dependence of diffusion coefficient was not considered, although it might be important for double-diffusion convection. In the simplified model with the fixed boundary melting temperature was fixed instead of being calculated from phase diagram.

The basic physics that controls solidification front shape formation is as follows. Due to the large separation between the liquidus and the solidus, there is a wide variation of composition through the boundary layer adjacent to the interface. Cooling from below and the segregation at the solid-melt interface of the heavier HgTe-rich solute each tend to suppress convection. However, the thermal conductivity of the solid is a factor of 8 times smaller then the melt (see table 1) and there is a resulting thermal short circuit through the ampoule (fused silica); this results in curved isotherms in this region as the heat cannot travel parallel to the axis within the center of the sample. The interface is therefore curved and, due to the thermal and solutal convection is neither an isotherm nor a line of isoconcentration. Double diffusion also contributes to the mass transport. In the present study, the numerical model is used to consider both these source of mass transport.

2. MATHEMATICAL MODEL AND NUMERICAL PROCEDURE

The main features of the model are double-diffusion convection in the melt and solidification. The set of steady state Navier-Stokes equations in Boussinesq approximation along with energy and solutal balance equations are used [6]. In the following **u** is melt convection velocity, **R** is sample pulling velocity (assumed at the steady state to be equal to crystal growth velocity), **p** - pressure, ρ - density, **g** -microgravity acceleration, β_T and β_C - volumetric expansion coefficients due temperature and concentration change respectively, $\mathbf{T_0}$ and $\mathbf{C_0}$ -reference temperature and concentration, μ - dynamic viscosity, **D** - mass diffusion coefficient, **k** - thermal conductivity, $\mathbf{C_p}$ - specific heat at constant pressure. Furthermore indexes "**solid**" and "**melt**" are used to refer to solidified and molten parts of the sample.

Momentum conservation equation (1)

$$\rho(u\nabla u) = -\nabla p + \mu\Delta u + \rho g[1 - \beta_T(T - T_0) + \beta_C(C - C_0)]$$

Mass conservation equation (Boussinesq approximation) (2)

$$\nabla u = 0$$

Energy conservation equation (3)

$$\rho C_p(u\nabla T) = \nabla(k\nabla T)$$

Species conservation equation (4)

$$u\nabla C = D\Delta C$$

The boundary conditions incorporate major physical assumptions in order to describe solidification of an unknown interface between molten and solidified HgCdTe. These phase change boundary conditions are as follows.

The melting temperature is determined by (5)

$$T_{melt} = T_{solid} = T_0(C_0) + m(C)C_{melt}$$

where (6)

$$m(C) = \frac{dT}{dC}$$

The heat balance on the interface, including latent heat release (L) is (7)

$$k_{melt}\nabla T_{melt}\cdot\vec{n} - k_{solid}\nabla T_{solid}\cdot\vec{n} = \rho_{solid}L\left(R - \frac{dS}{dt}\right)\cdot\vec{n}$$

Here t stands for pseudo-time, i.e. artificial melting time, used in the model to allow interface adjustment in accordance with temperature field and phase diagram. Notation n is unit vector normal to the interface.

The balance of the mass flux across interface is (8)

$$\rho_{melt}\left(u - \frac{dS}{dt}\right)\cdot\vec{n} = \rho_{solid}\left(R - \frac{dS}{dt}\right)\cdot\vec{n}$$

The no-slip boundary condition at the interface is (9)

$$(u - R)\times\vec{n} = 0$$

The mass balance for solute transport across the interface is (10)

$$\frac{\rho_{melt}}{\rho_{solid}}D_{melt}\nabla C_{melt}\cdot\vec{n} - D_{solid}\nabla C_{solid}\cdot\vec{n}$$

$$= C_{solid}\left(R - \frac{dS}{dt}\right)\cdot\vec{n} - C_{melt}\left(u - \frac{dS}{dt}\right)\cdot\vec{n}$$

(11)

The chemical equilibrium on the interface is (12)

$$C_{solid} = \kappa_{segregation}(C)C_{melt}$$

where (13)

$$\kappa_{segregation}(C) = \frac{Solidus(C)}{Liquidus(C)}$$

To perform actual calculations initial temperature and solutal field, convection velocities and interface position are required. In order to obtain a steady state solution of the problem (1-4) with boundary

conditions (5-11) a three step numerical procedure was used. On the first computational step the position of interface was flat and fixed, and so variable S = 0. Initial zero velocity field and constant initial distribution of temperature and concentration were used to obtain the solution of double-diffusion convection problem in two-dimensional area with fixed boundaries, that satisfies temperature boundary conditions obtained from global numerical model of AADSF furnace or using available measured temperature profile. This solution was used as initial conditions during the second step, when variable S was released and the interface shape was obtained with proper adjustment of the computational mesh. A final third step was required to obtain a convergent solution for all variables involved. Two-dimensional 9-node quadrilateral finite elements were implemented. Due to strong nonlinearity of the problem, a relaxation factor value as high as 0.9 was used for surface elevation variable S. A first-order upwinding numerical scheme was used. This ensures suppression of "wiggles", a typical problem caused by inadequate mesh density to resolve strong gradients of concentration. Further details on finite element implementation of the model can be found elsewhere [6]. For parametric studies a simplified model was used. The major simplification was the elimination of independent variable S with appropriate boundary conditions on the fixed solid/ melt interface.

3. NUMERICAL TEST PROBLEM: DOUBLE-DIFFUSION CONVECTION

In order to verify the numerical approach and choice of numerical parameters, such as mesh size and relaxation factors, the following problem was considered [9]. Double-diffusion convection governed by set of equations 1-4 occurs in a two-dimensional enclosure which is heated and salt rich at the bottom. This is a a case of opposing or counteracting flow, so that as the heat impact tends to start convection, the salt introduction from below tends to suppress it. It is also known as a "diffusive" regime, as the component with a higher diffusivity (heat) has a destabilizing effect, while the component with a lower diffusivity (salt) has a stabilizing effect on the local density gradient. Instead of the complicated boundary conditions 5-11, representing crystal growth in the region with the unknown boundary, a straightforward set of boundary conditions apply. Constant temperature and salinity on the top and the bottom of enclosure are determined by the (14)

$$y = 1 \qquad T = T_0 \qquad C = C_0$$

$$y = 0 \qquad T = T_1 > T_0 \qquad C = C_1 > C_0$$

while the isolated vertical boundaries of enclosure are (15)

$$x = 1, 0 \qquad \frac{\partial T}{\partial y} = 0$$

$$x = 1, 0 \qquad \frac{\partial C}{\partial y} = 0$$

In this case the following non dimensional parameters, which control fluid behavior can be introduced.Thermal and solutal Rayleigh numbers, based on enclosure height H and top to bottom differences of temperature and salt are as follows

$$Ra_T = \frac{(T_1 - T_0) \cdot \beta_T \cdot g \cdot H^3}{k_T \cdot \nu} \qquad Ra_C = \frac{(C_1 - C_0) \cdot \beta_C \cdot g \cdot H^3}{k_C \cdot \nu}$$

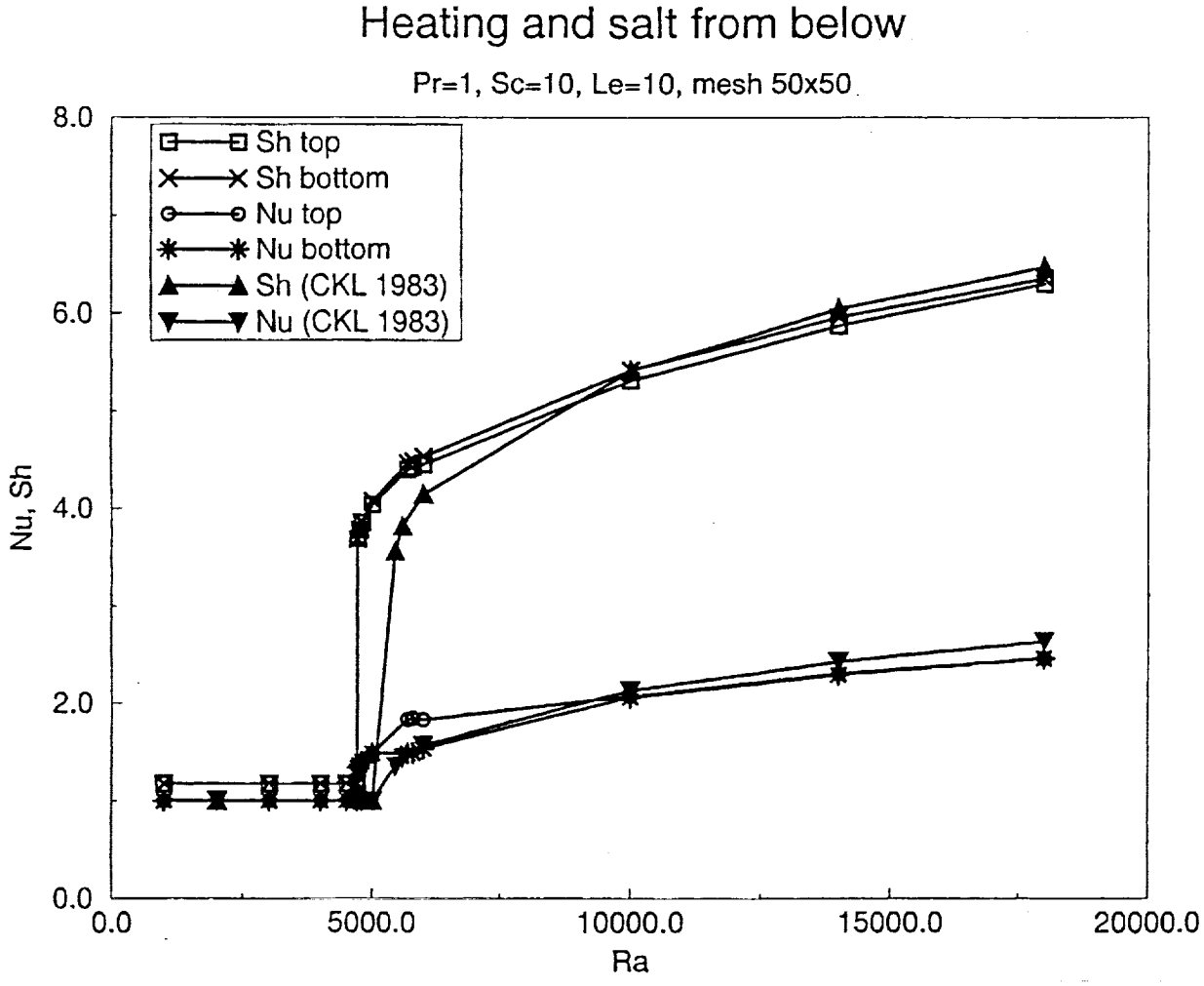

Figure 1.

Nusselt and Sherwood number dependence versus thermal Rayleigh number.Results of test problem appears in agreement with data from[9].

Here k_T and k_C - are thermal and mass diffusivity, respectively and ν is kinematic viscosity. The complete set of nondimesional parameters for this problem include also Prandtl and Lewis numbers. Geometry is characterized by aspect ratio.

$$Pr = \frac{\nu}{k_T} \qquad Le = \frac{k_T}{k_C} \qquad \frac{H}{L} = 1$$

To monitor convection influence on heat transfer we will use an overall Nusselt number at vertical walls

$$Nu = \int_0^H Nu_y dy \qquad where \qquad Nu_y = -\frac{H}{T_1 - T_0}\left(\frac{\partial T}{\partial y}\right)_{wall}$$

Similarly the impact of convection on solutal flux is characterized by overall Sherwood number

$$Sh = \int_0^H Sh_y dy \qquad where \qquad Sh_y = -\frac{H}{C_1 - C_0}\left(\frac{\partial C}{\partial y}\right)_{wall}$$

In order to perform comparison with published[9] results the nondimensional parameters where fixed, as follows: Ra_C=2000, Pr=1, Le=10, H/L=1. Thermal Rayleigh number was varied in wide range from 2000 to 18000 in order to determine the critical thermal Rayleigh number, when convection occurs. Results presented on fig 1, indicate good agreement with data from[9].

4. RESULTS AND DISCUSSION

Two complimentary solutions are presented here.

The first one is based on the complete model described in section 2. In this case typical distribution of temperature field along with pattern of melt flow is presented on fig2a. For comparison experimental photograph featuring "quenched" interface is presented on fig 2b. Good agreement in shape is mainly due proper choice of thermal conductivities of solidified and molten material as well as silica ampoule thermal conductivity and wall thickness. The relevant material and system parameters are presented in the tables 1-3. This is the case, the strict vertical orientation of the sample manifests itself in a symmetrical pattern of the flow. In other simulated cases deviation from the vertical of only 1 degree cases loss of symmetry and formation of one cell pattern of convection. These cases are featured in the video film. The shape of interface closely fits and is almost the same for various levels of gravity. This strongly suggests that convection in the melt virtually has no effect on solidification interface curvature in this particular case. Further efforts are required to investigate this finding in more detail. It should be noted, that simulation of this problem using non-dimensional parameters, like Rayleigh number, can be confusing in this case, as the driving force for convection is not a vertical or a simple radial gradient, but rather a radial temperature gradient created by the curvature of the solidification front. Otherwise the cooling of the melt from below and rejection of the heavier component (HgTe) would suppress convection. In this case both the shape of and concentration distribution along the interface are of major interest. Radial distribution of concentration and temperature are presented on fig 3. The radial variation in concentration is only in fair agreement with experimental observation. It appears, that the calculated temperature radial variation is about 7°C less than expected from the experimental observed variation of 20 °C.

The second set of solutions is based on simplified model with fixed solid / melt interface. Parametric study of maximum convection velocity depending on microgravity conditions is presented on fig 4a and 4b. Geometry of the sample and temperature boundary conditions was taken from experiment SLI-413. While material properties was the same as in former case, the system parameters was different, as shown in table 3. Figure 4a features convection velocity dependence on microgravity amplitude. Figure 4b presents the same data depending on gravity vector angle to sample axis. It is clear, that the maximum velocity of convection occurs, when ampoule is inclined at 90^0, while if ampoule is strictly vertical convection is less by factor of 50%. These data strongly suggest, that in order to reduce convection in the melt, vertical orientation of the

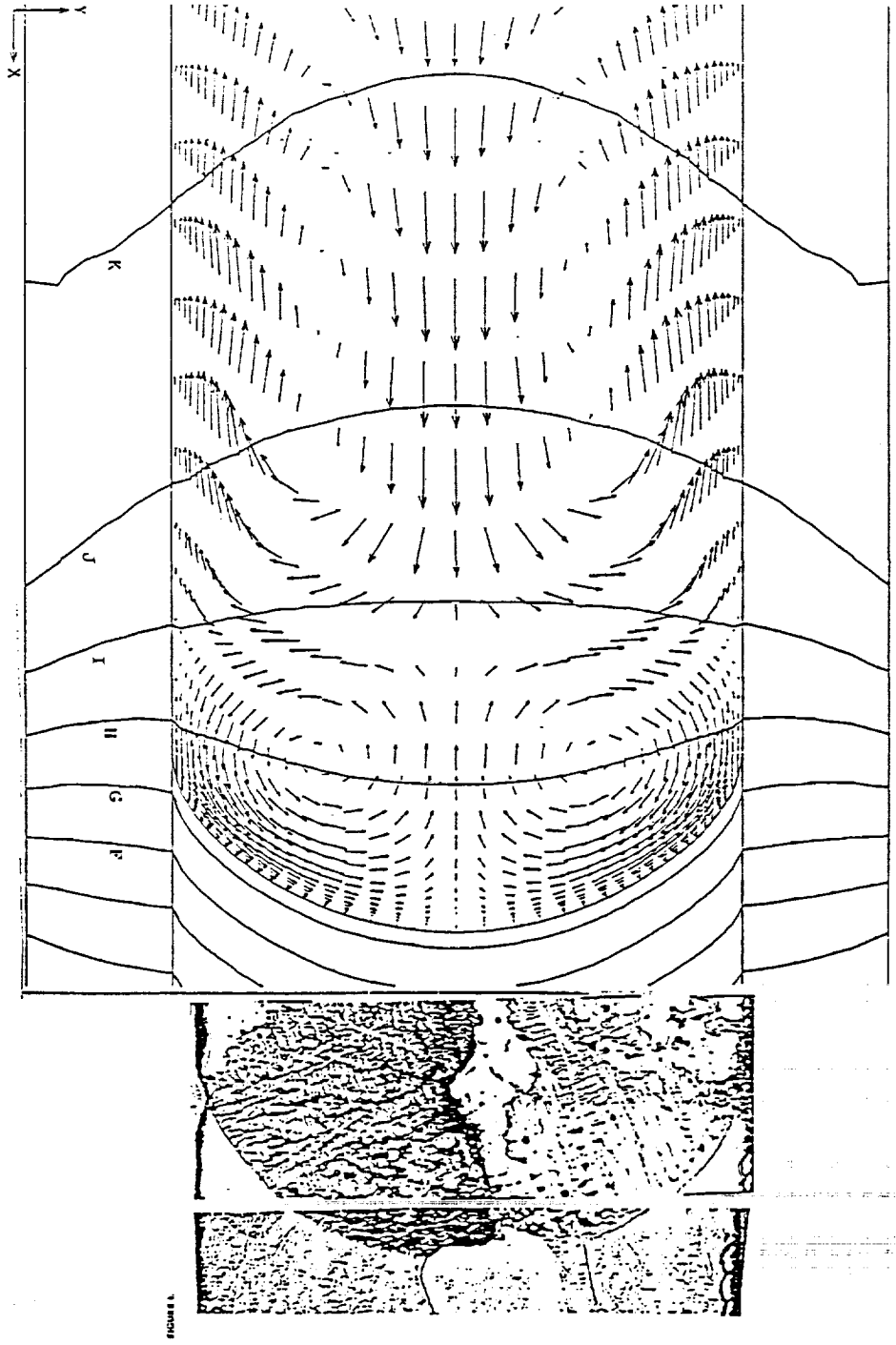

Figure 2.

a) Temperature field and convection patterns in the case of strict vertical orientation of the sample.

b) Experimental photograph of the interface shape. Case MCT-16Q.

Table 1. HgCdTe thermophysical property data

Thermal conductivity (solid)	0.291	W / °K m
Thermal conductivity (melt)	1.96	W / °K m
Density (solid)	7630	kg / m^3
Density (melt)	7550	kg / m^3
Specific heat (solid)	177	J / °K kg
Specific heat (melt)	257	J / °K kg
Kinematic viscosity	1.08×10^{-7}	m^2 / s
Latent heat	130000	J / kg
Thermal expansion coefficient	1.5×10^{-4}	$°K^{-1}$
Solutal expansion coefficient	0.3	$°K^{-1}$
Diffusion coefficient of CdTe	5.5×10^{-9}	m^2 / s
Melting temperature (liquidus)	$944.09 + 671.46 \times C - 375.07 \times C^2 + 110.54 \times C^3$	°K
Segregation coefficient	$4.7 - 15.9 \times C + 39.3 \times C^2 - 59.1 \times C^3 + 46.7 \times C^4 - 14.7 \times C^5$	

Table 2. Ampoule (Quartz) thermophysical property data

Thermal conductivity	2.5	W / °K m
Density	2200	kg / m^3
Specific heat	1050	J / °K kg

Table 3. System data

Case	SL-413	MCT-16Q	
Sample radius	3.9	3.9	mm
Sample length	110	138	mm
Ampoule outer radius	5.9	5.9	mm
Pulling velocity	2.0×10^{-7}	2.0×10^{-7}	m / s
Cold heater temperature	312	360	°C
Hot heater temperature	827	846	°C
CdTe initial concentration	0.152	0.2	

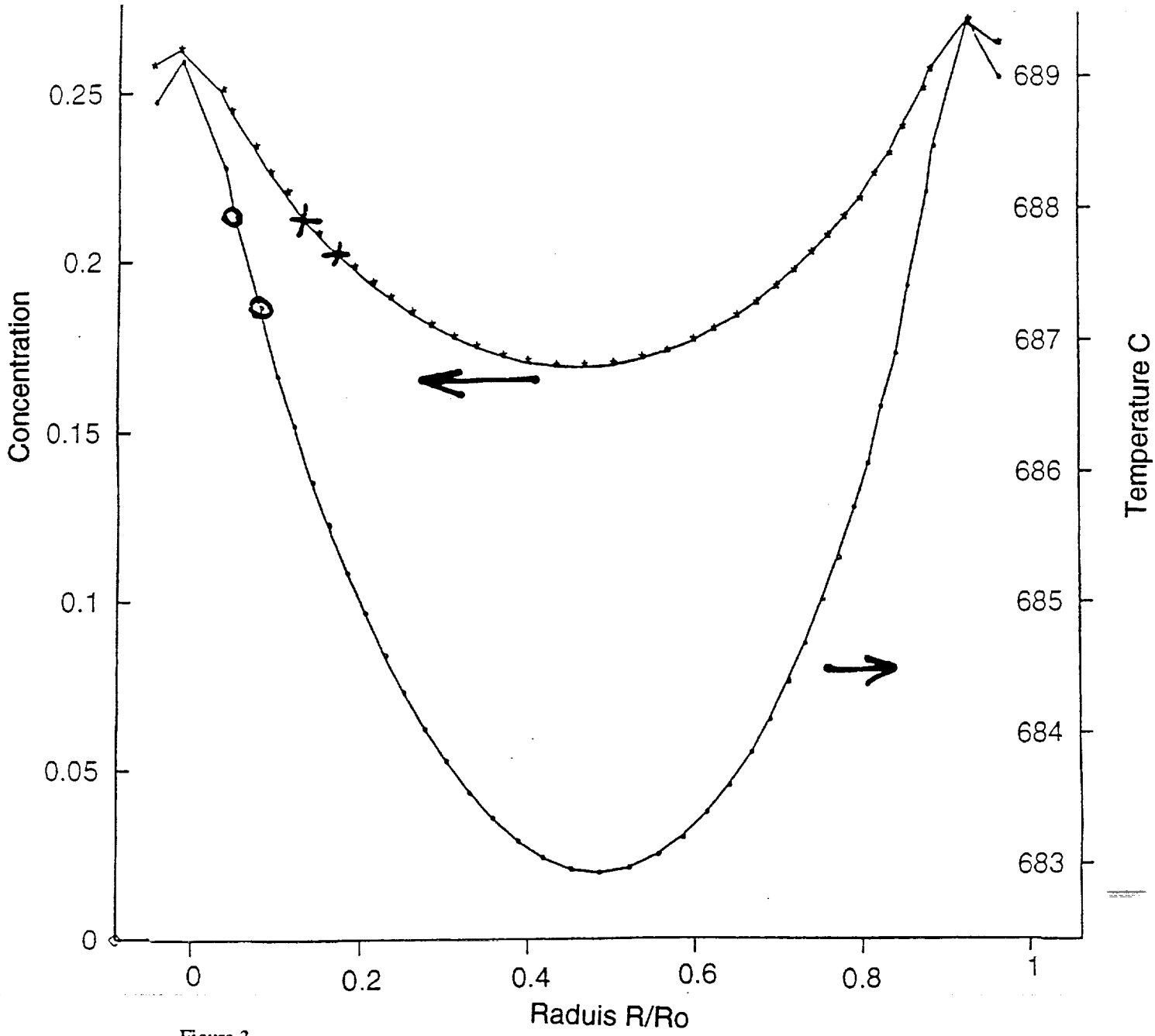

Figure 3.

Concentration and temperature distribution on the solidification interface. Crosses - concentration distribution (axis on the left). Circles - temperature distribution (axis on the right).

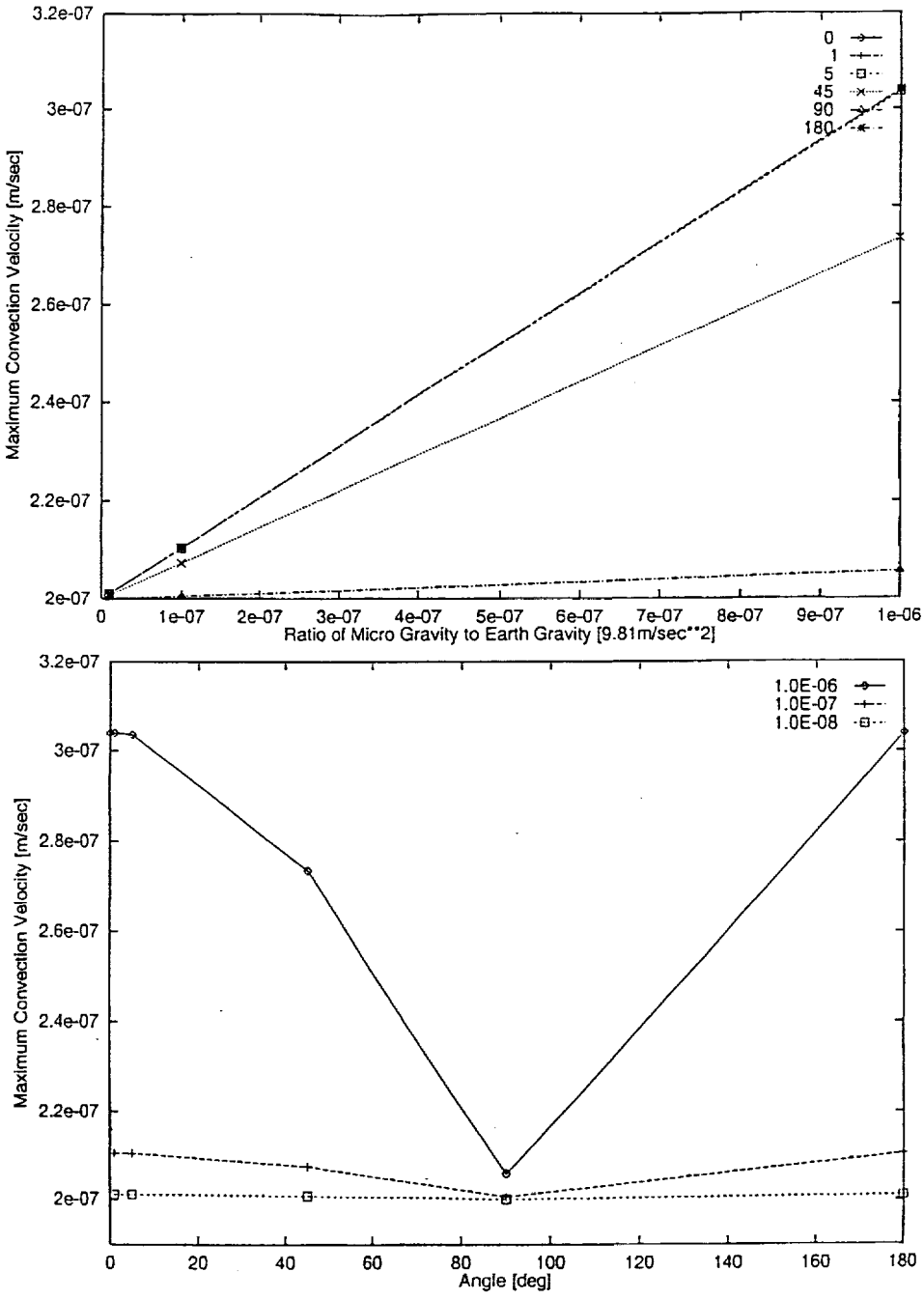

Figure 4.

a) Maximum convection velocity as function of microgravity acceleration amplitude.

b) Maximum convection velocity as function of gravity vector angle to sample axis. Angle of 90 degree corresponds to the strict vertical orientation of the sample.

ampoule is of utmost importance. This is valid till gravity level of order 10^{-6} of gravity on Earth. However at very low gravity, of order 10^{-7} and 10^{-8} of earth gravity the tilt of the ampoule has much less effect.

5. CONCUSIONS

Prediction of solidification interface shape and flow pattern in molten HgCdTe for various gravity conditions are available using a 2-D model of melt convection and solidification. This model utilizes temperature boundary conditions from results of modeling of heat transfer in AADSF furnace, and incorporates all basic modes of heat transfer, such as conduction, convection and radiation. Alternatively, a measured experimental temperature profile can be used.

It appears that crystal/melt interface shape, as well as concentration distribution on the interface depend primarily on heat flow and concentration distribution in close vicinity of interface. The models ability to predict correctly the interface shape and concentration distribution heavily depends on known material properties, such as conductivity and segregation coefficient.

Maximum convection velocity in the ampoule is extremely sensitive to gravity vector orientation and can be reduced at least by factor of 50% if vertical orientation of ampoule is strictly observed. This conclusion is valid to microgravity level of about 10^{-7} compared to earth gravity. If microgravity is lower than this level convection in the melt is not anymore sensitive to the ampoule orientation.

ACKNOWLEDGEMENTS

The authors thank James B. Hargrave for instant software support and help in video film production. The authors thank Dr. Narayanan Ramachandran for suggesting numerical test problem for double-diffusion convection. The work was supported by the Microgravity Science and Applications Division of the National Aeronautics and Space Administration and by National Research Council Research Associateship Programs.

REFERENCES

1. D.H.Kim and R.A.Brown, "Models for convection and segregation in the growth of HgCdTe by the vertical Bridgman method", *J.Crystal Growth* **96**, pp. 609-627, 1989.
2. D.H.Kim and R.A.Brown, "Modelling of the dynamics of HgCdTe growth by the vertical Bridgman method", *J.Crystal Growth* **114**, pp. 411-434, 1991.
3. Yu.V.Apanovich and E.D. Ljumkis, "The numerical simulation of heat and mass transfer during growth of a binary system by the travelling heater method", *J.Crystal Growth* **110**, pp. 839-854, 1991.
4. A.V. Bune, D.C. Gillies and S.L. Lehoczky, "Optimization of bulk HgCdTe growth in a directional solidification furnace by numerical simulation", *Mat.Res.Soc.Symp. Proc.* **Vol. 398**, pp. 139-144, 1996.
5. A.V. Bune, D.C. Gillies and S.L. Lehoczky, "Evaluation of temperature gradient in Advanced automated Directional Solidification Furnace (AADSF) by numerical simulation", *SPIE* **Vol. 2809**, pp. 196-204, 1996.
6. FIDAP Theory Manual Version 7.0, Fluid Dynamics International, Inc., Evanston, Illinois, 1993.
7. F.R. Szofran and S.L. Lehoczky, "The Pseudobinary HgTe-CdTe phase diagram", *J.Elec.Mats*, **10**, pp. 1131-1150, 1981.
8. K. Mazuruk, C.-H. Su, S.L. Lehoczky and F. Rosenberger, "Novel oscillating cup viscometer - application to molten HgTe and $Hg_{0.8}Cd_{0.2}Te$", *J. Appl. Phys*, **77**(10), pp. 5098-5102, 1995.
9. S.-M. Chang, S.A.Korpela and Y.Lee, "Double diffusive convection in the diffusive regime", Applied Scientific Research **39**, pp.301-319, 1982.